JAM CM Journal of Applied Mathematics and Computational Mechanics 2025, 24(3), 5-17
www.amcm.pcz.pl p-ISSN 2299-9965
DOI: 10.17512/jamcm.2025.3.01 e-ISSN 2353-0588

NUMERICAL MODELLING OF SANDWICH PANELS SUBJECTED TO FIRE CONDITIONS

El Mehdi Ablaoui[1], Jolanta Pozorska[2], Zbigniew Pozorski[1]
Paweł Roszkowski[3], Michał Malendowski[1]

[1] Institute of Structural Analysis, Poznan University of Technology, Poznań, Poland
[2] Institute of Mathematics, Poznan University of Technology, Poznań, Poland
[3] Fire Research Department, Building Research Institute, Warsaw, Poland
elmehdi.ablaoui@doctorate.put.poznan.pl, jolanta.pozorska@put.poznan.pl
zbigniew.pozorski@put.poznan.pl, p.roszkowski@itb.pl, michal.malendowski@put.poznan.pl

Received: 30 July 2025; Accepted: 9 September 2025

Abstract. The paper addresses the problem of numerical modelling of sandwich panels exposed to fire temperatures. A complex spatial model is presented that takes into account the variation of material parameters with temperature. A cohesive interaction is defined between the panel layers, for which damage initiation and propagation criteria are provided. Thermal conductivity and radiation are also determined for this interaction and possible separation. In addition, support conditions simulating the experimental test conditions were defined. A combination of classical contact and point interactions using connectors is used for this purpose. The model is used to simulate fire exposure and compared with experimental results. The obtained results confirm that the model is suitable for predicting the general trend of panel behaviour during fire.

MSC 2010: *74A10, 74A50, 74F05, 74M15, 74R20, 74S05, 74-05, 80-05, 80A20, 80M10*
Keywords: *numerical modelling, computational mechanics, sandwich panels, fire conditions*

1. Introduction

Sandwich panels are commonly used in construction as walls or roofs [1], but similar sandwich structures are also used in advanced industries [2, 3]. The panels consist of two thin but rigid facings and a thick but shear-deformable core. One of the most interesting, yet challenging, issues related to sandwich panels is their behaviour under fire-related temperatures. Under high temperatures, the core layer, designed as a thermal barrier, deteriorates significantly, while the face layers are subjected to thermal stresses that can lead to delamination or structural failure. The coupling of mechanical and thermal fields makes it difficult to accurately predict the mechanical behaviour and structural integrity of panels.

To address this challenge, numerical modelling approaches that incorporate both thermal and mechanical effects have been developed. Coupled thermo-mechanical analyses have proven effective in capturing the intricate behavior of materials under thermal loading, including simulating the displacement and failure of sandwich panels during fire exposure [4]. The problem of the response of a sandwich panel exposed to fire or another source of elevated temperature on one of its surfaces was addressed in [5], where the first-order shear strain theory was applied. This paper takes into account the dependence of the mechanical properties of materials on temperature. The nonlinear behaviour of sandwich panels with compliant cores with temperature-dependent mechanical properties was presented in [6], but a more complex approach based on a higher-order sandwich panel was used. A thermomechanical model predicting the temperature distribution, decomposition, softening, and failure of sandwich structures in fire was developed in [7]. This model takes into account thermochemical decomposition in the facings and the effect of thermal resistance on interfacial contacts. A thermomechanical model predicting the temperature increase, softening rate, failure time, and failure mechanism of a sandwich composite under combined tensile loading and unilateral fire heating was presented in [8]. This is one of the few studies that considered the case of tensile loading. A general three-dimensional numerical model based on the finite element method suitable for predicting the thermomechanical behaviour of reinforced concrete load-bearing walls exposed to fire was presented in [9]. The proposed model takes into account critical parameters determining the fire resistance of walls, such as the wall slenderness ratio, support constraints, and temperature-dependent properties. In [10], experimental results and material models were described. A finite element (FE) model was developed using commercial advanced software to investigate the fire resistance of composite sandwich panels. The developed model was validated with available fire test data. A critical review of progress in the structural analysis and modelling of composite materials in fire was presented in [11]. The authors indicated that further analysis and validation based on experimental data is necessary. In particular, the effect of fire-induced damage, such as delamination cracks and skin-core debonding, on the heat flow process should be considered.

Despite the above-mentioned findings, advantages, and applications of sandwich panel systems, very few studies in the literature address their fire resistance behaviour at full scale or under real conditions. On the other hand, predicting thermomechanical behaviour is crucial for improving the design and safety of sandwich panel systems subjected to fire [12]. Therefore, this paper presents an attempt to apply advanced numerical methods to simulate the behaviour of sandwich panels under fire temperature exposure.

2. Problem formulation

Sandwich panels used in construction are susceptible to structural degradation in the event of a fire due to high temperatures, changes in material properties, and,

consequently, debonding at the adhesive interface between the steel facings and the mineral wool core. However, predicting the behaviour of sandwich panels in a fire is very important. From a safety perspective, the key factor is the time during which a wall made of panels retains its load-bearing capacity, integrity, and insulation. Due to the complex effects of thermal impact described above, standardized fire tests are performed to predict panel behaviour. The difficulty lies in the fact that as a result of single (and expensive) tests, it is difficult to clearly determine the influence of any factor on the final result of the laboratory test. The solution is to develop a numerical model that can accurately describe the behaviour of panels exposed to fire temperatures. Such a model must certainly take into account coupled thermal and mechanical fields as well as the dependence of material properties on temperature. The development of a reliable model will allow for the analysis of the impact of model parameters on the behaviour of walls made of panels.

This study addresses this challenge by developing a finite element model based on cohesive interactions, with clearly defined boundary conditions, and validated against full-scale fire resistance experiments. The objective is to simulate displacements and delamination phenomena under thermal exposure, with emphasis on adhesive layer degradation and joint behaviour under varying thermal loads.

3. Experimental tests

Fire tests were performed to validate the numerical model. The tests were conducted at the Fire Research Department of the Building Research Institute in Warsaw. The experimental programme described in this study involved two large-scale sandwich panel walls. Mineral wool was used as the core material of the panels. The tests were carried out in accordance with the procedures specified in [13-15].

The walls examined were at least 3.00 m wide and high, constructed of 150 mm thick sandwich panels attached to a non-combustible, solid support structure. The horizontal panel arrangement, which is common for mineral wool core panels, was used for the test. During the test, one wall surface is exposed to a temperature that increases with test time according to a standard relationship. On the unexposed side of the wall, displacements perpendicular to the wall and temperatures were measured at specific points. Locations of temperature (1-17) and displacement (A-J) measurement points were presented in Figure 1b. Figure 2a presents the unexposed side, before the test, and Figure 2b shows the heated side, after the test.

The supporting structure was made of 240 mm thick aerated concrete blocks with a density of 600 kg/m^3, together with a reinforced concrete lintel with a cross-section of 240 mm × 240 mm. Hot-rolled L80 × 80 × 8 steel profiles were attached to the bottom and side edges of the supporting structure using self-drilling steel anchors. The top edge of the panel wall was left free. The gap between the free edge of the panel and the supporting structure was filled with 50 mm thick mineral wool. The sandwich panels were attached to L-shaped steel profiles using self-drilling screws with a diameter of 5.5 mm (see Fig. 1a). Dilatations were made between

the aerated concrete blocks and the panels; 25 mm wide on the sides and 10 mm wide on the bottom. The dilatations were filled with mineral wool. In addition, the L80 × 80 × 8 steel profiles were protected from temperature exposure using mineral wool. The tests were performed as described in Table 1.

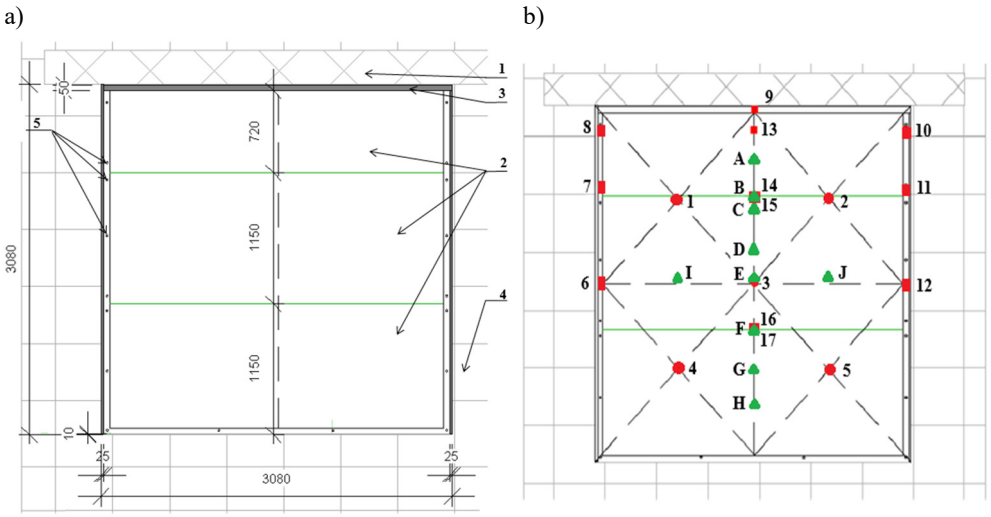

Fig. 1. Front view of the assembled sandwich panel wall in Test 1: a) components of the wall: 1 – reinforced concrete lintel, 2 – sandwich panels with a mineral wool core, 3 – free edge filled with insulation material, 4 – aerated concrete blocks, 5 – self-drilling screws with a diameter of 5.5 mm and a length of 190 mm, b) locations of temperature (1-17) and displacement (A-J) measurement points

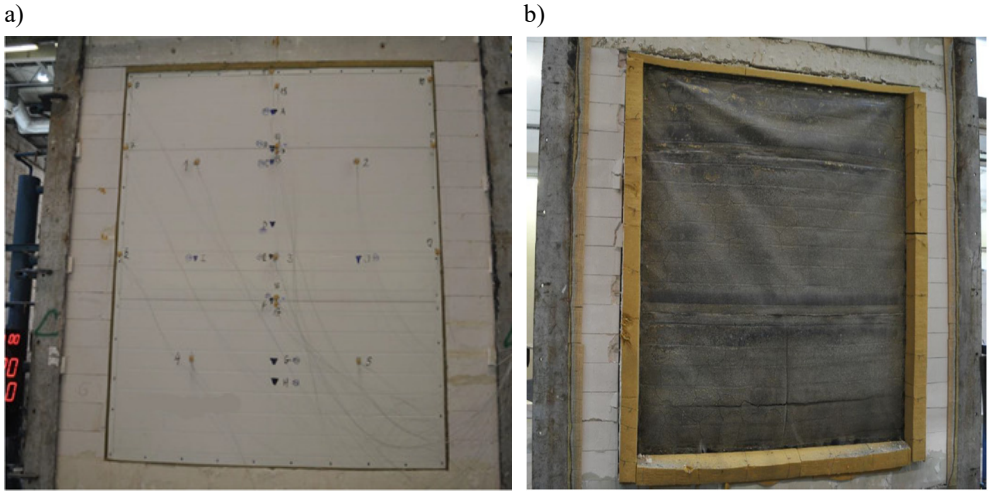

Fig. 2. Experimental test: a) initial setup of the tested wall – unheated side of the wall, b) heated side at the end of the test

Table 1. Description of the experimental large-scale tests

Experiment	Duration	Sandwich panel wall	Panel composition	Panel arrangement
Test 1	3 h 02 min = 10,920 s	Thickness: 150 mm width: 3080 mm, height: 3080 mm (panels 3020 mm, bottom insulation 10 mm and top insulation 50 mm)	Steel facings: 0.50 mm (S280 GD + Z115 and polyester coating); Core: mineral wool, 150 mm, 100 kg/m^3; Adhesive: one-component 0.26 kg/m^2	Horizontal arrangement of three panels (1150 mm + 1150 mm + 720 mm)
Test 2	3 h 22 min = 12,120 s	Thickness: 150 mm width: 3050 mm, height: 3010 mm (panels 2950 mm, bottom insulation 10 mm and top insulation 50 mm)	Steel facings: 0.50 mm (S280 GD + Z115 and polyester coating); Core: mineral wool, 150 mm, 100 kg/m^3; Adhesive: one-component 0.26 kg/m^2	Horizontal arrangement of three panels (1150 mm + 1150 mm + 650 mm)

4. Numerical model

This section presents a numerical model prepared using ABAQUS software [16], which is based on the finite element method (FEM). The model defined in 3-D space was developed in two similar variants corresponding to the multi-scale experimental tests described above: Test 1 and Test 2. The core of the sandwich panels was modelled using solid elements, and the steel facings using shell elements. The model, which takes into account the coupling of thermal and mechanical fields, allows for the analysis of temperature distribution, displacements, deformations, and damage mechanisms. The model considers core-facing interactions, interactions between panels, and local effects occurring at the connections between panels and the supporting structure. The presented approach includes bolted connections, spring elements for describing the connections between adjacent panels, interaction-contact definitions for bonding, and cohesive contact formulations taking into account damage initiation and evolution. Furthermore, thermal conductivity and radiative heat transfer are considered, as well as precise geometric definitions.

In all models, the material properties of steel (S280GD + Z) and mineral wool with a density of 100 kg/m^3 were defined. The thermal properties of steel were obtained from [17], the mechanical properties from [18], and the thermal data of mineral wool from [19]. The mechanical properties of mineral wool reflect its low stiffness, which is consistent with its function as non-load-bearing insulation [20]. It exhibits a thermal expansion coefficient of approximately 7×10^{-6} 1/°C [21], which ensures dimensional stability. The yield stress decreases from approximately 30 MPa at 21.1 °C [22] to 5 MPa at 500 °C, reaching a value close to zero at 850 °C due to fiber softening.

4.1. Thermal boundary conditions

Thermal boundary conditions were applied to simulate heat fluxes arising from convection and radiation. Convection was represented by two surface film conditions. For the region at room temperature, a film coefficient of 9 W/m^2 K was applied, with a constant ambient temperature of 21.1 °C and instantaneous amplitude, as prescribed in [23]. For the fire-exposed surface, a film coefficient of 25 W/m^2 K was used in accordance with the convective heat transfer coefficients specified in [23] for fire resistance analysis. Radiative heat transfer was also considered. For the surface at room temperature, an emissivity of 0.7 was used following the guidelines of [23] regarding thermal assessments of construction materials. The same emissivity value was assigned to the surface exposed to fire, according to [18], which defines the fire resistance test parameters. These boundary conditions were essential to accurately replicate the experimental thermal loading conditions within the thermal analysis. The thermal loading in the numerical model was established by applying the ISO 834 standard fire curve as the reference heating profile, which represents the nominal thermal boundary condition.

4.2. Mechanical boundary conditions

The sandwich panels are supported by L80 × 80 × 8 steel profiles. For simplicity, it was assumed that the steel profile surface in contact with the aerated concrete block structure is rigidly connected. A more complex, contact-type connection was defined between the L-profiles and the surfaces of adjacent panel facings. A hard contact was established in the normal direction, and a friction coefficient of 0.3 was defined in the tangential direction.

The sandwich panels are attached to the structure using mechanical connectors, as shown in Figure 1a. To simulate this type of interaction, a bushing connector was used in the numerical model. At each location where a real self-drilling screw was present, a connection between two points was defined; one point was located on the surface of the L80 × 80 × 8 profile, and the other point was located on the outer facing of the sandwich panel. Using the coupling function, the displacements of the surrounding region were assigned to the point located on the facing, thus avoiding highly localized deformations [24]. The bushing connector allows for the determination of stiffness associated with the relative displacement of the points it connects.

Since the sandwich panels had a thickness of L = 150 mm and the steel self-drilling screws used had a diameter of 5.5 mm, corresponding to the cross-sectional area of the connector A = 23.76 mm^2 and the moment of inertia I = 44.92 mm^4, for the modulus of elasticity E = 210 GPa, the stiffness of the connection in the axial direction was determined as

$$K_x = \frac{EA}{L} = 33262 \text{ N/mm}, \tag{1}$$

and in the transverse directions as

$$K_y = K_z = \frac{3EI}{L^3} = 8.385 \text{ N/mm}. \tag{2}$$

It's worth noting that the library of connectors available in Abaqus is very extensive, allowing the definition of nonlinear constitutive relationships. Furthermore, the coupling function used in the model includes the option to account for thermal expansion, which proved very helpful in this case.

The interaction between adjacent panels still needs to be defined. Adjacent panels are not mechanically connected, but the panel edges have a special profile that fits together using a tongue-and-groove principle. After fitting the adjacent panels and applying a seal, the connection creates tight thermal insulation and prevents the passage of flame and smoke. Of course, the actual geometry of the panels can be represented in a three-dimensional numerical model, but it is quite complex and therefore significantly affects the numerical problem (the number of elements, nodes, and interactions). To overcome these types of problems, certain simplifications are often used. In the presented model, as in [4], instead of introducing precise geometry of the longitudinal edges of the panels, elastic connections between the facings are used, as shown in Figure 3. The connections are applied at a single point, in the middle of the panel span. The stiffness of the two springs connecting the facings in their plane limits the mutual displacement of the panels in their plane and the rotation of the panels relative to each other. Additionally, an elastic connection is used to limit the lateral displacement of the panels relative to each other. The stiffness of the elastic connections can be determined experimentally or based on independent numerical simulations. In the presented model, the stiffness of the elastic connections between the panels is set at 1 kN/mm.

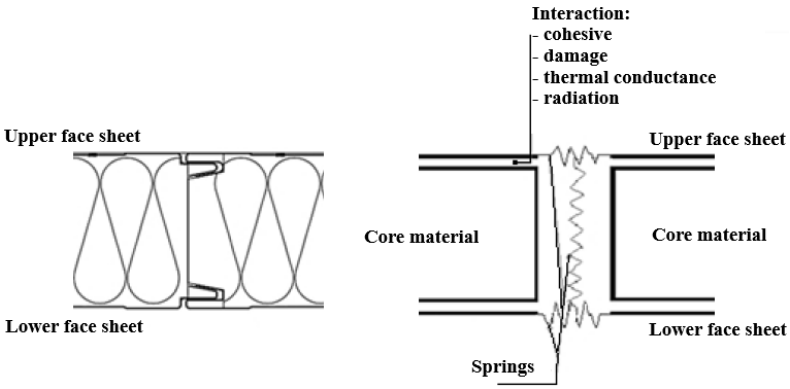

Fig. 3. Schematic representation of simplified joint connection and interface properties with interaction details

4.3. Modelling the interface between the face sheets and the core

The steel facings of sandwich panels are bonded to the mineral wool core in a continuous production process using a polyurethane adhesive. This bonding is often modelled as a perfect TIE interaction, where the facing displacements match the core displacements. The conducted experimental study showed that this assumption is far from realistic. Therefore, in the presented approach, the adhesive bond was modelled using the cohesive interaction (see, Figure 3). This method is based on the traction-separation law, and additionally allows for defining damage initiation and development. Cohesive interactions were defined to capture the interfacial degradation observed during early fire exposure (at approximately 250 °C for 50 seconds), which challenges the assumption of perfect adhesion. A maximum separation criterion was used to initiate damage. Damage development after initiation was governed by a linear softening law.

The model of cohesive interaction includes three components: the traction-separation law, damage initiation criterion, and the damage evolution law. The traction--separation law describes the elastic behaviour of the interface. It is defined by the stiffness matrix **K** that relates the traction vector **T** to the separation vector **δ**:

$$\mathbf{T} = \mathbf{K}\,\boldsymbol{\delta}. \tag{3}$$

The stiffness matrix, the separation vector, and the traction vector are defined as:

$$\mathbf{K} = \begin{bmatrix} K_{nn} & 0 & 0 \\ 0 & K_{ss} & 0 \\ 0 & 0 & K_{tt} \end{bmatrix}, \quad \boldsymbol{\delta} = \begin{bmatrix} \delta_{nn} \\ \delta_{ss} \\ \delta_{tt} \end{bmatrix}, \quad \mathbf{T} = \begin{bmatrix} T_{nn} \\ T_{ss} \\ T_{tt} \end{bmatrix} \tag{4}$$

where K_{nn}, K_{ss}, and K_{tt} represent the normal, first tangential, and second tangential stiffnesses, respectively; δ_{nn}, δ_{ss}, and δ_{tt} correspond to the normal, first tangential, and second tangential separations; and T_{nn}, T_{ss}, and T_{tt} are traction components in the respective directions.

Damage initiation was assumed to occur once the maximum effective separation δ_{eff} exceeded a critical threshold δ_0, which was defined as:

$$\delta_{eff} = max(|\delta_{nn}|, |\delta_{ss}|, |\delta_{tt}|) \geq \delta_0. \tag{5}$$

Once the threshold δ_0 was reached, stiffness degradation was controlled by a scalar damage variable D, which varied linearly from 0 to 1 between δ_0 and the final separation δ_f:

$$D = \frac{\delta_{eff} - \delta_0}{\delta_f - \delta_0}, \quad \text{for } \delta_0 \leq \delta_{eff} \leq \delta_f. \tag{6}$$

At degradation described by parameter D, the stiffnesses K_{nn}, K_{ss}, and K_{tt} are reduced by the multiplier $(1 - D)$. Thus, at full degradation ($D = 1$), the stiffness

is equal to 0. These formulations allowed accurate representation of progressive delamination under mixed-mode loading conditions.

To determine the parameters necessary to model the interface, two steel clamps were prepared and connected with a polyurethane adhesive used in the production of sandwich panels with a mineral wool core. A two-component adhesive filled with calcium carbonate was used. The steel elements were glued together on the production line of one of the manufacturers during its normal operation. The adhesive was spread using a moving comb that was part of the production line. After the adhesive was applied, the samples were transferred to an incubator, where they were cured at 60 °C for 20 minutes to simulate the conditions in the production line tunnel. After 6 hours of bonding, the prepared steel-adhesive-steel specimens, measuring 10 cm × 10 cm, were subjected to tensile testing using an Instron ElectroPuls E10000 machine at room temperature 21 °C (Fig. 4a).

The force-displacement curves (Fig. 4b) exhibited an initial disturbance of 0.4 mm, corresponding to the removal of the load system clearance, followed by linear elastic behaviour up to failure. Some differences in the graphs in the range of 0.5-1.5 mm may result from imperfections in the distribution and thickness of the applied adhesive layer. From the linear range of the force-displacement relationship, the average stiffness of the adhesive joint was determined to be 0.591 MPa/mm. For the assumed linear constitutive relationship, for an average joint load capacity of 7.528 kN, failure is achieved at a displacement of δ_0 = 1.27 mm. Because full failure occurs quite suddenly, final separation was defined as 1.40 mm – 10 % higher than δ_0. Shear properties of the interface were assumed to be equivalent to tensile properties, given the comparable strength behaviour of the adhesive.

Temperature dependence of the interface parameters was incorporated by adjusting stiffness and final separation. Interface stiffness declined from 0.591 MPa/mm at 21 °C to zero at 250 °C, based on the previously conducted experimental tests. Final separations increased from 1.40 mm (21 °C) to 3.50 mm (250 °C), reflecting increased ductility under heat.

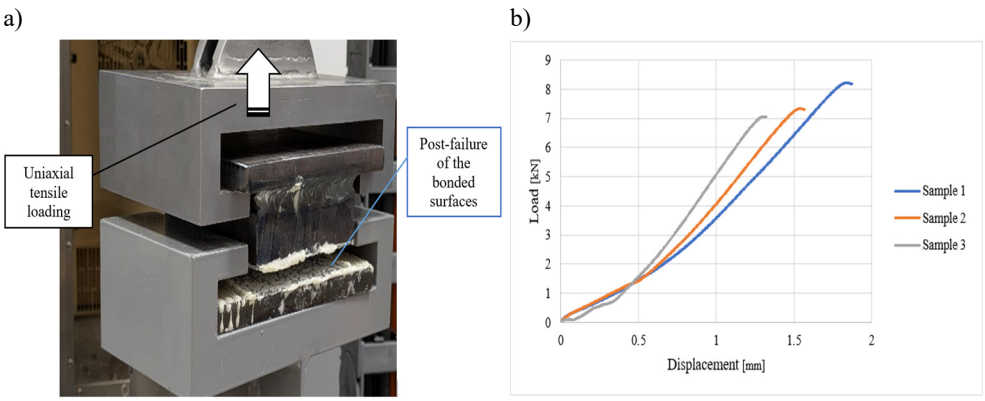

Fig. 4. Steel plate specimens bonded with polyurethane adhesive and their tensile response: a) testing with uniaxial tension machine, b) load-displacement curves

5. Modelling of thermal conductance and radiation

To fully define the interactions at the interface, it is necessary to determine the thermal contact conductance and radiative heat transfer. The thermal contact conductance was therefore defined as a function of the interfacial clearance, allowing for the reduction in heat transfer efficiency as the gap between the steel sheet and the mineral wool core increases to be accounted for. In parallel, radiative heat transfer was modelled using surface emissivity values and clearance-dependent view factors.

The convective heat transfer coefficient at the interface between steel and mineral wool was defined as 35 $W/m^2 K$ according to [23]. This value reflects the expected thermal performance of the interface, considering limited effective contact area and the conduction suppression resulting from the fibrous structure of mineral wool. To capture the thermal behavior at complete separation, the conductance was defined as a function of separation. When the separation exceeded 1.40 mm, the conductance is reduced to 0 $W/m^2 K$ because physical contact was no longer present.

In the case of separation, radiative heat transfer becomes the dominant interfacial mechanism. The radiative exchange between the steel sheet and the mineral wool core is governed by the gap geometry, represented by the radiative view factor. The view factor was set to 1 when the gap exceeded 1.40 mm, corresponding to full radiative exposure. In the case of full contact, the view factor was set to 0, indicating complete suppression of radiative exchange. This methodology enabled a physically realistic transition conductivity and radiation.

6. Results and discussion

This section presents a comparative evaluation of numerical simulations and experimental data from Tests 1 and 2, focusing on displacement responses at selected measurement points. The aim is to assess the agreement between the numerical predictions and the observed experimental results.

Measurement Points A, D, E, and H were selected based on their strategic locations within the panel configuration, as depicted in Figure 1b. Points A, D, and E are situated at the approximate centres of individual panels, representing the typical mid-span response of each panel section. Point H is located at the geometric centre of the entire wall assembly and captures the overall structural behaviour.

At Points A and D (Fig. 5a and 5b), displacement-time curves revealed a characteristic initial elastic response transitioning to time-dependent deformation. FEM predictions captured the qualitative behaviour in both tests, confirming the validity of the implemented interface parameters under moderate thermal influence.

At Point E (Fig. 5c), located near the mid-span of the lower panel, more substantial deviations were observed. Particularly in Test 2, the FEM simulation significantly underpredicted the final displacement, with discrepancies exceeding 20 mm. This divergence is attributed to the elevated thermal gradient and adhesive softening effects experienced in this region. The pronounced displacement in the experimental

data suggests nonlinear damage accumulation and thermal relaxation effects, which cannot be easily simulated using a linear cohesive law. It is worth emphasizing here the very large differences in the displacements obtained in Test 1 and Test 2, which indicate the high unpredictability of the panels' behaviour under the influence of fire temperatures.

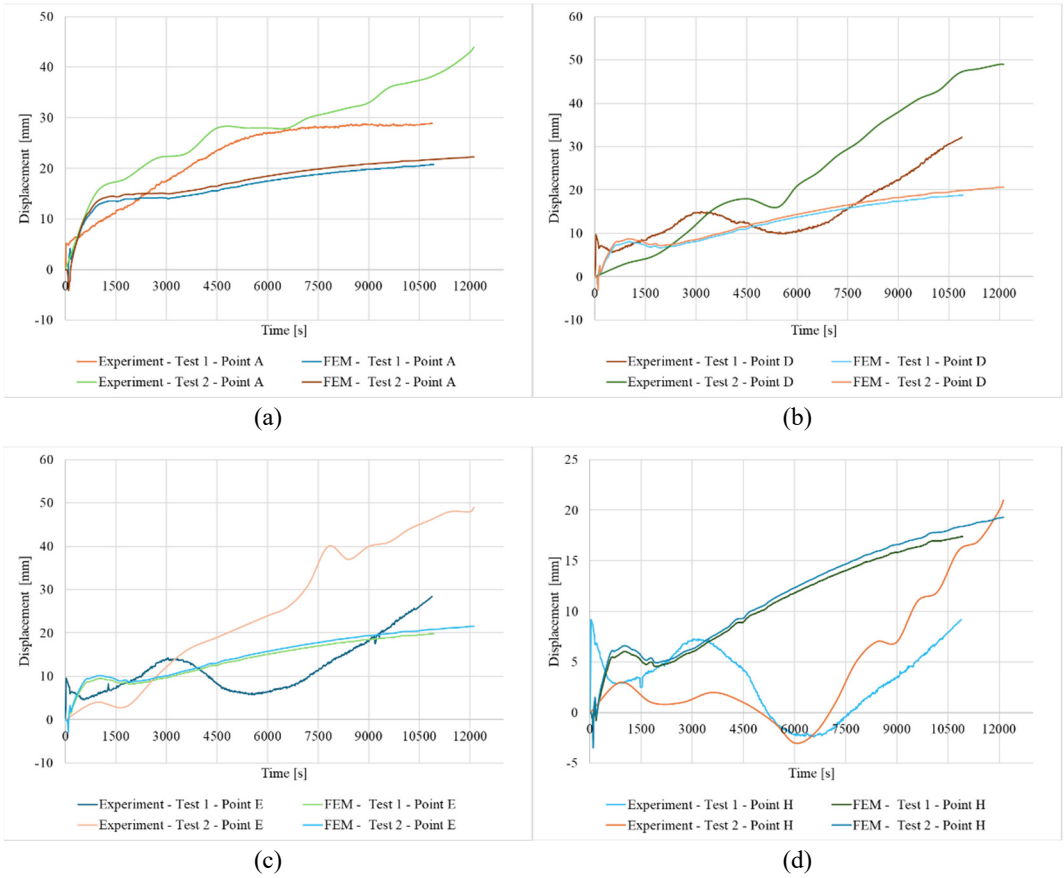

Fig. 5. Comparison of experimental and FEM displacement-time responses at measurement points A, D, E, H

At point H (Fig. 5d), located in the centre of the tested wall, the FEM results differ from the experimental results. Although the model reflected the general growth trend, it failed to capture the transient relaxation phase observed experimentally in the time interval 3000-7000 s. The observed discrepancy may be due to significant limitations of the interface model used and the processes occurring inside the sandwich panels, which are very difficult to identify and verify. Nevertheless, the overall agreement confirms the partial adequacy of the model under mixed thermomechanical loading conditions.

7. Conclusions

This paper presents a complex numerical model for modelling the behaviour of a sandwich panel wall exposed to fire temperatures. The model reflects the actual panel support conditions, including panel attachment using fasteners. The temperature dependence of properties was considered when defining the materials comprising the sandwich panels. A key consideration was the assumption of cohesive interaction between the facings and the core. This enabled the definition of damage initiation and its subsequent propagation criteria. Thermal contact conductance and radiative heat transfer were also defined. The presented model offers extensive capabilities for simulating phenomena occurring during fire exposure.

The developed numerical model was used to compare simulation results with those from experimental studies. The analysed thermal load was consistent with the ISO 834 standard fire curve. The numerical results enabled the observation of the variability of the coupled thermal-mechanical fields over time. It turned out that the actual behaviour of the panels is highly unpredictable. Local disturbances, instabilities, and temporary changes in displacement direction can be observed, primarily attributed to non-uniform thermal gradients, adhesion degradation, and complex interactions between the panels and the supporting structure. FEM results showed smoother displacement fields. Despite some discrepancies, the developed numerical model can be considered effective in determining the general displacement trends of sandwich panels exposed to fire temperatures. This allows for the prediction of the panels' fire resistance. Future work should focus on experimental studies covering the phenomena of conduction and radiation in the early phase of facing-core separation, as well as the dependence of the interface properties on temperature.

References

[1] Davies, J.M. (2001). *Lightweight Sandwich Construction*. Oxford: Blackwell Science.

[2] Ginot, M., Bouvet, C., Castanié, B., Serra, J., & Mahuet, N. (2023). Local buckling on large sandwich panels used in light aviation: experimental setup and failure scenarios. *Composite Structures*, *304*, 116439.

[3] Ren, X., Zhang, S., & Wu, Z. (2023). A strategy resisting wrinkling of sandwich structures reinforced using functionally-graded carbon nanotubes. *Chinese Journal of Aeronautics*, *36*, 243-255.

[4] de Boer, J.G.G.M., Hofmeyer, H., Maljaars, J., & van Herpen, R. A. P. (2019). Two-way coupled CFD fire and thermomechanical FE analyses of a self-supporting sandwich panel façade system. *Fire Safety Journal*, *105*, 154-168.

[5] Birman, V., Kardomateas, G.A., Simitses, G.J., & Li, R. (2006). Response of a sandwich panel subject to fire or elevated temperature on one of the surfaces. *Composites Part A: Applied Science and Manufacturing* , *37*(7), 981-988.

[6] Frostig, Y., & Thomsen, O.T. (2014). *Thermomechanical Nonlinear Response of Sandwich Panels*. In Hetnarski, R.B. (eds), Encyclopedia of Thermal Stresses, Springer, Dordrecht, 5999-6011.

[7] Looyeh, M.R.E., Rados, K., & Bettess, P. (2001). Thermomechanical response of sandwich panels to fire. *Finite Elements in Analysis and Design*, *37*(11), 913-927.

[8] Anjang, A., Chevali, V.S., Kandare, E., Mouritz, A. P., & Feih, S. (2014). Tension modelling and testing of sandwich composites in fire. *Composite Structures*, *113*, 437-445.

[9] Kumar, P., & Kodur, V.K.R. (2017). Modeling the behavior of load bearing concrete walls under fire exposure. *Construction and Building Materials*, *154*, 993-1003.

[10] Upasiri, I.R., Konthesigha, K.M.C., Nanayakkara, S.M.A., Poologanathan, K., Gatheeshgar, P., & Nuwanthika, D. (2021). Finite element analysis of lightweight composite sandwich panels exposed to fire. *Journal of Building Engineering*, *40*, 102329.

[11] Mouritz, A.P., Feih, S., Kandare, E., Mathys, Z., Gibson, A.G., Des Jardin, P.E., Case, S.W., & Lattimer, B.Y. (2009). Review of fire structural modelling of polymer composites. *Composites Part A: Applied Science and Manufacturing*, *40*(12), 1800-1814.

[12] Studziński, R., Pozorski, Z., Błaszczuk, J. (2015). Optimal support systems of sandwich panels. *Journal of Engineering Mechanics*, *141*(3), 04014133, 1-8.

[13] European Committee for Standardization, EN 14509:2013 Self-supporting double skin metal faced insulating panels – Factory made products – Specifications. CEN, Brussels, 2013.

[14] European Committee for Standardization, EN 1364-1:2015 Fire resistance tests for non-loadbearing elements – Part 1: Walls. CEN, Brussels, 2015.

[15] European Committee for Standardization, EN 1363-1:2020 Fire resistance tests – Part 1: General requirements. CEN, Brussels, 2020.

[16] Dassault Systèmes. (2016). ABAQUS 6.14 documentation. Providence, RI: Dassault Systèmes Simulia Corp.

[17] Craveiro, H.D., Rodrigues, J.P.C., Santiago, A., & Laím, L. (2016). Review of the high temperature mechanical and thermal properties of the steels used in cold-formed steel structures – The case of the S280GD+Z steel. *Thin-Walled Structures*, *98*, 154-168.

[18] European Committee for Standardization, EN 1993-1-2: Eurocode 3 – Design of Steel Structures – Part 1-2: General Rules – Structural Fire Design. CEN, Brussels, 2005.

[19] Ablaoui, E.M., Malendowski, M., Szymkuc, W., & Pozorski, Z. (2023). Determination of thermal properties of mineral wool required for the safety analysis of sandwich panels subjected to fire loads. *Materials*, *16*(17), 5852.

[20] Chuda-Kowalska, M., Pozorski, Z., Garstecki, A. (2010). Experimental determination of shear rigidity of sandwich panels with soft core, *10th International Conference Modern Building Materials, Structures and Techniques*. Vilnius, Lithuania, 19-21 May 2010, 56-63.

[21] American Society of Heating, Refrigerating and Air-Conditioning Engineers, Inc., ASHRAE Handbook – Fundamentals (SI Edition) (2017). Chapter 26: Heat, Air, and Moisture Control in Building Assemblies.

[22] Xu, Q., Hofmeyer, H., Maljaars, J., & van Herpen, R.A.P. (2024). Full-scale fire resistance testing and two-scale simulations of sandwich panels with connections. *Fire Technology*, *60*, 2461-2488.

[23] European Committee for Standardization, EN 1991-1-2: Eurocode 1 – Actions on Structures – Part 1-2: General Actions – Actions on Structures Exposed to Fire. CEN, Brussels, 2002.

[24] Pozorski, Z., & Pozorska, J. (2016). Stress redistribution at the support of a transversely loaded sandwich panel. *Advances in Mechanics: Theoretical, Computational and Interdisciplinary Issues:* Proceedings of the 3rd Polish Congress of Mechanics (PCM) and 21st International Conference on Computer Methods in Mechanics (CMM). Gdansk, Poland, 8-11 September 2015, 485-488.